Magnetism in ZnO nanowire with Fe/Co codoping: First-principles density functional calculations

S. Ghosh,[1,*] Q. Wang,[2] G. P. Das,[1] and P. Jena[2]
[1]*Department of Materials Science, Indian Association for the Cultivation of Science, Jadavpur, Kolkata 700032, India*
[2]*Department of Physics, Virginia Commonwealth University, Richmond, Virginia 23284, USA*
(Received 14 April 2010; published 23 June 2010)

Using first-principles density functional calculations, at both generalized gradient approximation (GGA) and GGA+U levels we have investigated the electronic structure and magnetic properties of Fe/Co codoped ZnO nanowire. Here we have addressed some of the key issues such as, the preferable sites that Fe/Co can occupy, the coupling mechanism, and role of defects in coupling. We found that the spin alignment between the transition-metal atoms depends on their location. When Fe and Co atoms are nearest neighbors on the outer surface of the nanowire along [0001] direction is the lowest energy configuration with ferrimagnetic (FiM) ground state. At GGA level of description ferromagnetic ordering is observed when impurity atoms sit at surface and subsurface interface forming Fe-O-Co magnetic path, however at GGA+U level of description antiferromagnetic superexchange interaction dominates and all configuration leads to FiM ground state. GGA+U are found to give more realistic description of electronics structure of Fe/Co codoped ZnO nanowire. Interestingly Fe-V_O-Co defect configurations formed by removing the O atom from Fe-O-Co magnetic path are ferromagnetic when Fe-Co separation is less than 2.596 at GGA and 2.801 Å at GGA+U irrespective of the location of transition ions. We have also found that Co atom has a tendency to form clusters around Fe atom leading to inhomogeneous doping concentrations. O vacancy is found to be crucial in case of promoting ferromagnetism in this system. Two competing factors are the Ruderman-Kittel-Kasuya-Yosida (RKKY) type of exchange interaction in bulk environment due to O vacancy and direct exchange interaction of carriers due to Fe-V_O-Co defect configuration on the surface.

DOI: 10.1103/PhysRevB.81.235215 PACS number(s): 75.75.−c, 36.40.Cg, 73.22.−f, 75.50.Pp

I. INTRODUCTION

Spintronics is currently an active area of research because spin-based multifunctional electronic device has several advantages over the conventional charge-based devices regarding data-processing speed, nonvolatility, higher integration densities, etc.[1] The impending need to obtain such device has led to growing interest in developing and designing spintronic materials. Dilute magnetic semiconductors are promising candidates in this regard. In particular, ZnO-based materials have been receiving considerable attention due to its abundance and environment-friendly nature and also due to its potential as a suitable optoelectronic material[2,3] with a wide band gap (~3.34 eV) and high excitation binding energy of 60 meV. The magnetic, electronic, optical, and electrochemical properties of ZnO offer the unique possibility to create multifunctional integrated device for sensing, processing, and actuating functions in one monolithic structure. With the advancement of experimental techniques interest in zero-dimensional and one-dimensional (1D) ZnO-based materials as building blocks of new electronic and spintronic devices is rapidly increasing. The study of the effect of dimensionality on magnetic, optical, and mechanical properties is therefore important not only for technological applications but also to strengthen our basic understanding in low dimensions.

Recently transition-metal (TM) doped 1D ZnO nanowires of varying diameter were grown by various experimental techniques and ferromagnetic (FM) ordering has been found at a range of temperatures from low to room temperature.[4–9] Considerable effort has also been devoted for introducing two different 3d-TM impurities into ZnO matrix in order to explore the effect of codoping on transition temperature. Cho *et al.*[10] reported room-temperature ferromagnetism in ZnO films codoped with Fe and Co (Fe/Co), which were prepared using a reactive magnetron cosputtering technique. Liu *et al.*[6] successfully synthesized (Fe/Co) codoped 1D ZnO naowires via chemical vapor deposition growth method and observed Curie temperature was higher than 300 K. Previous theoretical study by Park and Min[11] on bulk $Zn_{1-x}(FeCo)_xO$ indicated that there is no indication of charge transfer between Fe and Co. They suggested that double exchange mechanism will not be effective for observed ferromagnetism and one needs to invoke other exchange mechanism between Fe and Co. Defects such as O vacancy or Zn interstitial (n-type defect) and Zn vacancy (p-type defect) seem to play important role and need to be investigated.

We have carried out first-principles investigation of electronic structure and magnetic properties of (Fe/Co) codoped ZnO nanowire. Here we have addressed some of the key issues such as (a) what are the preferable sites that Fe and Co atoms occupy? (b) What is the appropriate coupling mechanism between Fe and Co? (c) What is the role of defects in the coupling between Fe and Co? The present results also demonstrate the role of surface curvature and the radial confinement of the electrons on magnetic coupling in codoped ZnO nanowires.

II. THEORETICAL METHOD

The ZnO nanowire has been constructed from a $(7\times7\times2)$ ZnO wurtzite supercell by removing Zn and O atoms from outside the circle of 1 nm diameter and replacing it with vacuum space shown in Fig. 1(a). The nanowire thus

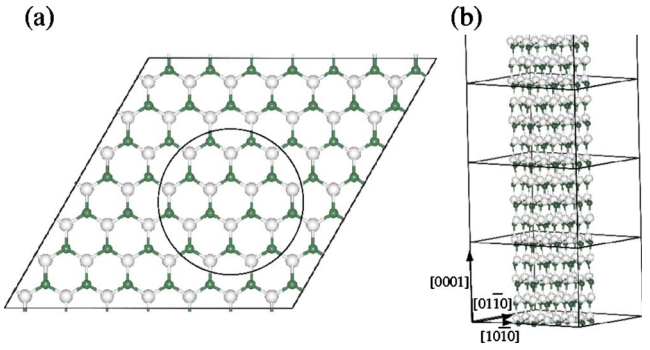

FIG. 1. (Color online) (a) Top view of a $7\times7\times2$ ZnO supercell (0001) plane having wurtzite structure. (b) A ZnO nanowire supercell ($Zn_{48}O_{48}$) which extends to infinite along the [0001] direction. The white (lighter) spheres are Zn and dark green (gray) small spheres are O.

created contains 96 atoms ($Zn_{48}O_{48}$) with a vacuum space of 12.997 and 13.011 Å along the [10$\bar{1}$0] and [01$\bar{1}$0] directions, respectively, thereby ensuring that wires in neighboring supercells do not interact with reach other. Along the [0001] direction the wire extends to infinity through Bloch periodicity as shown in Fig. 1(b).[12]

In order to simulate codoping, we have replaced two Zn atoms with one Fe and one Co atom which corresponds to ~2% Fe and ~2% Co, i.e., ~4% Fe/Co codoped ZnO nanowire. Since the preferred sites for Fe and Co atoms are not known *a priori*, we have tried 14 different configurations that can be categorized into four groups: for Group-I, where both Fe and Co are in the bulk environment, i.e., having tetrahedral coordination. Group-II, where both Fe and Co lie on the cylindrical surface, i.e., having one broken bond. Group-III, where Fe lies on the surface and Co is at the subsurface and Group-IV, where Co lies on the surface and Fe at the subsurface. Figure 2 shows these four categories, Group-I and Group-II, each having three possible configurations and

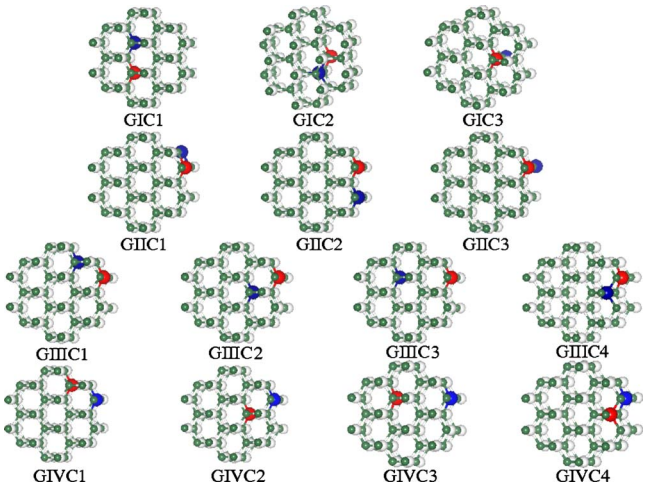

FIG. 2. (Color online) The schematic representation of 14 configurations of $Zn_{46}Fe_1Co_1O_{48}$ nanowire supercell. The white (lighter) spheres are Zn, dark green (gray) small spheres are O, the red (gray) large spheres are Fe, and the blue (dark gray) large spheres are Co.

Group-III and Group-IV having four possible configurations leading to a total of 14 configurations. These configurations simulate different possible Fe-Co and Fe-O-Co distances as well as Fe-O-Co bond angles. In Group-III and Group-IV we have taken into account the situations where Fe and Co occupy the surface and the subsurface (in GIII) and vice versa (in GIV). Here we have not considered the effect of surface passivation, i.e., the surface have dangling bonds when we have determined the preferable sites and magnetic coupling between TM atoms.

For each of these configurations we have computed the total energies corresponding to both FM and ferrimagnetic (FiM) alignments of Fe and Co spins with full geometry optimization without any symmetry constraint. We have used spin polarized density functional theory[13] and generalized gradient approximation (GGA) (Ref. 14) for exchange and correlation. The calculations were carried out using the Vienna *ab initio* simulation package (VASP) and plane-wave basis set.[15] The projector augmented wave (PAW) potentials[16] were used for Zn, O, Fe, and Co. These potentials are known to be more accurate than the conventional or ultrasoft pseudopotentials in treating magnetic systems involving transition metals. The energy cutoff is set to 350 eV. Here we have taken soft oxygen PAW potential (PAW_GGA O_s 04May1998) where recommended minimum cutoff for oxygen is 250 eV. The accuracy of our calculations for ZnO system has been well established from our previous work.[12,17,18] The convergence in energy and force was set as 10^{-4} eV/Å and 10^{-3} eV/Å, respectively.

We approximated the exchange-correlation function with local spin density approximation (LSDA) and LSDA+U. It is well documented that LSDA underestimates the band gap, in case of ZnO despite having an experimental band gap of 3.34 eV, LSDA band gap are around 0.8 eV. This underestimation of band gap and absence d-d static correlation can lead to an uncorrected metallic description in case of TM doped semiconducting oxides. Recently some attempts were made to revisit TM doped ZnO with band-gap correction. Lany *et al.*[19] have achieved self-consistence band-gap correction by adding to the standard GGA+U Hamiltonian empirical nonlocal external potentials that depended on atomic type and the angular momentum. They pointed out that GGA and there +U extensions predict the absence of FM coupling in case of Co doped ZnO with electron doping where such coupling is expected or may predict FM coupling in case of Cr doped ZnO where such coupling may not be possible. When the band gap is corrected it turns out that both Co and Cr doped ZnO electron mediated FM is possible. In another study by Walsh *et al.*[20] investigated Co doped ZnO with using DFT+U s/d method to correct the band-gap error by applying a Coulomb U on both the s and d orbitals to further raise the band gap to 2.8 eV. They concluded that when band gap is corrected which leads to the correct location of unoccupied Co t_{2g} states to the n-type region of the conduction of ZnO and then FM can be achieved by reasonable electron doping concentration.

However in case of nanowire the band gap is expected to be large compare to bulk due to quantum confinement. Our calculated band gap for ZnO naowire is 1.14 eV. Density of states for pure ZnO nanowire shows the broad (~4–5 eV)

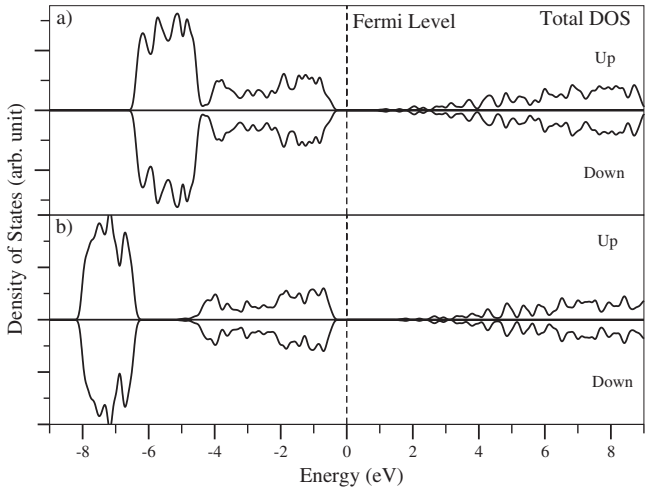

FIG. 3. Total density of states of pure ZnO nanowire obtained in (a) GGA description and (b) GGA+U description. Applying U =7 eV and J=1 eV to Zn d orbital it becomes more localized (~7–8 eV) and separated from O $2p$ states that has an indirect effect in raising the band gap as it has increased to 2.02 eV.

band just below the Fermi level (EF) which is due to O $2p$ states. Zn d state is just below O $2p$ states and in GGA level overlapping with the O bands. Applying U =7 eV and J=1 eV to Zn d orbital it becomes more localized (~7–8 eV) and separated from O $2p$ states that has an indirect effect in raising the band gap as it has increased to 2.02 eV (shown in Fig. 3). However it is still below the experimental bulk ZnO band gap, if we take the band-gap correction in account then the gap in ZnO nanowire is expected to be larger.

In this paper the computation has been done at both GGA and GGA+U_d levels. In GGA+U_d calculations we have used rotationally invariant "+U" formulation. We first varied U on both Co and Fe from 2 to 6 eV for the ground-state configuration, treating U as parameter, in order to find out how magnetic coupling is affected by the strength of the Coulomb correction. Finally we use U=3.5 eV for Fe d and U =2.8 eV for Co d for all the configurations as these values are reported to give the correct relative stability of different oxide semiconductors[19] and U=7 eV is used for Zn d, exchange parameter is set to the typical value of J=1 eV.

III. RESULTS AND DISCUSSIONS

We begin with a study of the relaxation of the atoms in the nanowire without Fe and Co incorporation. The effects of Co and Fe doping on the magnetic properties are then calculated by first keeping the doped nanowire in the unperturbed bulk geometry and then by allowing all the atoms (including Fe and Co) to relax. We find that in pure ZnO nanowire in wurtzite structure, relaxation of atomic positions is significant due to the large surface area. The total energy of the relaxed cell was found to be 6.712 eV lower in energy than the unrelaxed one at GGA level. This corresponds to an energy gain of 0.14 eV per Zn-O dimer. In bulk crystal, the calculated Zn-O bond length along the [001] direction is 1.993 Å while that between Zn and three O atoms in (0001) plane is 1.975 Å. In ZnO nanowire, the bond length changed to 1.888 Å for the surface atoms in [0001] direction and to 1.956 Å between the surface and subsurface layer atoms in (0001) plane of the $Zn_{48}O_{48}$ supercell. The relaxations of the atoms in the inner sites are much smaller than those on the outermost surface layer, as expected. The total electronic density of states (DOS) for pure ZnO nanowire using GGA and GGA+U, where U=7 eV is applied on Zn d orbital are plotted in Fig. 3, which reflects the system is semiconductor and nonmagnetic.

Now we discuss our results for different configurations of the Fe/Co codoped ZnO nanowire, carried out for both FM and FiM states at GGA level. The results are summarized in Table I. The configuration GIIC1, in which Fe and Co atoms are at nearest neighbors on the outer surface layer along [0001] direction of the ZnO nanowire, is found to be the lowest energy configuration. The difference in FiM and FM total energy ($\Delta E = E_{FiM} - E_{FM}$) is −0.175 eV, which indicates that the system is in FiM ground state.

Using the ground-state energy of GIIC1 as the reference, we have calculated the relative formation energy ($\Delta\varepsilon$) of other configurations and found that, GIIC2 and GIVC1 are the next two higher energy configurations with relative formation energies 0.112 eV and 0.122 eV, respectively. Here GIIC1 and GIIC2 represent the configuration where Fe and Co both are at surface while GIVC2 represents the configuration where Co at surface and Fe at subsurface. The Fe-Co distance corresponding to GIIC1, GIIC2, and GIVC1 configurations are 2.60 Å, 3.388 Å, and 2.478 Å, respectively. The corresponding ΔE values are −0.175, −0.132, and 0.119 eV. We also found that when Fe and Co atoms are in the bulk environment (GI configurations) and are at surface (GII configurations) the magnetic ground state is FiM and at large distance degenerate in energy (DE) while in case when Fe and Co atoms are at surface-inner surface environment (GIII and GIV) configurations FM is dominates over FiM. Thus the coupling is dependent not only on the relative separation between Fe-Co but also on the direction and location of the impurity atom, which is a unique manifestation in the nanowire.

In case of unpassivated pure ZnO naowire the cylindrical surface has dangling bonds. The bonding environment is different when Zn is replaced on the surface sites and at the subsurface/core site, in this case cylindrical surface has dangling bonds and surface is allowed to relax and then the corresponding energy gain is 0.14 eV per Zn-O dimer while in case of passivated pure ZnO nanowire due to fourfold coordination surface energy minimization will be less and location of the TM atoms in core expected to be enhanced. In case of unpassivated nanowire when Fe-Co is on the surface, is allowed to relax to minimize the strain effect and hence the surface substitution is preferred. Looking at the relative formation energies of GIIIC1, GIIIC2 and GIVC1, GIVC2 (given in Table I) it is clear that in case of surface-subsurface/core interface Co prefers to sit at the surface. The Co-Fe distance is reduced from 2.608 to 2.460 Å, when Co is on the surface and Fe is at the inner site.

In the last three columns of Table I, we have listed the magnetic moments on Fe and Co sites along with the in-

TABLE I. The energy difference ΔE between FiM and FM states ($\Delta E = E_{FiM} - E_{FM}$ in eV), the relative energy $\Delta\varepsilon$ (in eV) calculated with respect to the ground-state configuration GIIC1 with geometry optimization, the optimized Co-Fe and Fe-O and Co-O distances (in Å) and the magnetic moments (in μ_B) at Fe and Co, and the nearest-neighbor O atom for the configurations at GGA level given in Fig. 2. Here DE represents degenerate in energy. For DE situation both Fe-O and Co-O distances and magnetic moments on Fe,Co and the nearest-neighbor O atom are given for both FM and FiM magnetic states.

Configurations	ΔE	$\Delta\varepsilon$	Coupling	$d_{Fe\text{-}Co}$	$d_{Fe\text{-}O}$	$d_{Co\text{-}O}$	μ_{Fe}	μ_{Co}	μ_O
GIC1	−0.065	0.671	FiM	3.182	1.926	1.991	3.686	−2.414	0.074
GIC2	−0.014	0.688	FiM	3.167	1.928	2.001	3.697	−2.424	0.076
GIC3	0.002	0.752	DE	5.237	1.949	1.982	3.714	2.484	0.145
				5.251	1.946	1.986	3.695	−2.415	0.012
GIIC1	−0.175	0.000	FiM	2.605	1.847	1.803	3.220	−2.269	−0.066
GIIC2	−0.132	0.112	FiM	3.388	1.918	1.948	3.436	−2.417	0.040
GIIC3	0.002	0.210	DE	5.140	1.869	1.828	3.500	2.456	0.165
				5.130	1.868	1.827	3.50	−2.452	0.015
GIIIC1	0.001	0.279	DE	2.544	1.862	1.971	3.478	2.514	0.221
				2.903	1.857	1.918	3.426	−2.486	0.028
GIIIC2	0.081	0.309	FM	2.608	1.911	2.608	3.500	2.403	0.154
GIIIC3	0.015	0.429	FM	5.335	1.867	1.983	3.500	2.410	0.000
GIIIC4	−0.058	0.317	FiM	3.235	1.921	1.974	3.449	−2.516	0.014
GIVC1	0.119	0.122	FM	2.478	1.952	1.852	3.653	2.354	0.252
GIVC2	0.250	0.211	FM	2.460	2.022	1.905	3.526	2.470	0.171
GIVC3	0.016	0.521	FM	5.338	1.981	1.858	3.599	2.368	0.114
									0.022
GIVC4	−0.047	0.250	FiM	3.331	1.942	1.972	3.727	−2.361	0.005

duced moment on the neighboring O atom. In the ground state, i.e., the FiM configuration of GIIC1 the magnetic moment per supercell is 0.89 μ_B which is in agreement with experimental and previous theoretical studies.[11,21] Magnetic moments on Fe, Co, and O atoms (forming Fe-O-Co magnetic path) are 3.220 μ_B, −2.269 μ_B, and 0.074 μ_B, respectively. It is interesting to note that in case of FM ground-state configuration (such as GIIIC2, GIVC1, and GIVC2) the neighboring O atom linking Fe and Co is polarized ferromagnetically (positive magnetic moment) with respect to both Co and Fe while in case of FiM ground-state configurations (such as GIC1, GIC2, and GIIC2) the induced polarizations in O is antiferromagnetic (AFM) (negative magnetic moment) with respect to Co and ferromagnetic with respect to Fe.

Incorporating coulomb "*U*" at transitional metal *d* orbital can improve the electronic structure description of the system and to further confirm that the calculated magnetic coupling is not a consequence of the approximation to exchange and correlation potential, we have also performed GGA+*U* calculation for different *U* values in the range from 2 to 6 eV for the GGA ground-state configuration GIIC1. We found that the coupling strength gets reduced with increased *U* value but for GIIC1 configuration our qualitative conclusion remains unchanged, i.e., FiM coupling is lower in energy (as given in Table II) than FM. The values of local magnetic moments at Fe and Co sites increase with the Coulomb *U*: from 3.426 ($U=2$) to 3.691 ($U=6$) for Fe and from −2.441 ($U=2$) to −2.710 ($U=6$) for Co. Next we computed the energy difference between FM and FiM states for all the configurations (in groups GI, GII, GIII, and GIV) with incorporating *U* parameter to GGA, i.e., at GGA+*U* level ($U=3.5$ eV for Fe *d* and $U=2.8$ eV for Co *d*) to find out if the magnetic coupling remains same. In Fig. 4, we have plotted the ΔE ($E_{FiM} - E_{FM}$) for all configurations that we have considered here. GGA+*U* calculation alters the result signifi-

TABLE II. The energy difference ΔE between FiM and FM states ($\Delta E = E_{FiM} - E_{FM}$ in eV), the average moment at Fe, Co, and O forming Fe-O-Co magnetic path (in μ_B) calculated using GGA+*U* method for $Zn_{46}Fe_1Co_1O_{48}$ supercell in GIIC1 configuration and compared with GGA result.

$Zn_{46}Fe_1Co_1O_{48}$ (GIIC1)	GGA	$U_{Fe,Co}=2$	$U_{Fe,Co}=3$	$U_{Fe,Co}=4$	$U_{Fe,Co}=5$	$U_{Fe,Co}=6$	$U_{Fe}=3.5$, $U_{Co}=2.8$
ΔE	−0.175	−0.067	−0.058	−0.052	−0.043	−0.028	−0.054
μ_{Fe}	3.220	3.426	3.511	3.578	3.635	3.691	3.542
μ_{Co}	−2.269	−2.441	−2.537	−2.605	−2.661	−2.710	−2.524
μ_O	−0.066	−0.019	0.003	0.011	0.021	0.016	−0.012

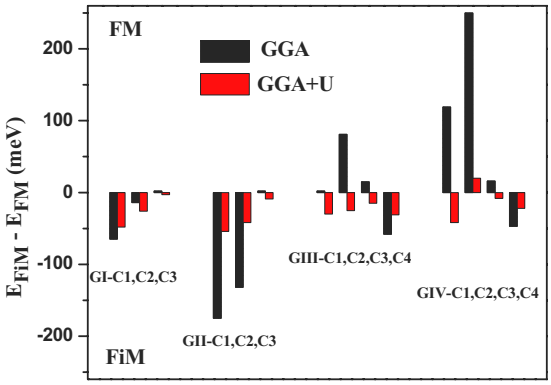

FIG. 4. (Color online) Magnetic exchange interaction energy ($\Delta E = E_{FiM} - E_{FM}$ in meV) for all the Fe/Co codoped configurations based on GGA calculation as shown with black filled bar and GGA+U calculation as shown as the red (dark gray) filled bar.

cantly. GGA calculation shows in case of surface-subsurface interface (GIII and GIV) first-nearest-neighbor interaction can lead to FM ground state. However in GGA+U consideration antiferromagnetic superexchange interaction dominates and all configuration leads to FiM ground state except GIVC2 which is weakly ferromagnetic.

In Fig. 5(a) total DOS of the ground state, i.e., GIIC1 in FiM configuration at GGA level has been shown. System has finite DOS at Fermi level and the system is half metallic in nature. The orbital resolved partial DOS at the Fe 3d, Co 3d, and O 2p are plotted in Fig. 5(c). Here we have not found any significant overlap in the DOS between O 2p and Co 3d/Fe 3d and O atom. This suggest that coupling is not mediated by O 2p orbital and therefore the observed FM cannot be described by double exchange mechanism. It is well known that at GGA level the band gap is underestimated, and in case of TM dopant in semiconducting host it also underestimates the static correlation in localized orbital, taking the two factors together electronic structure for this

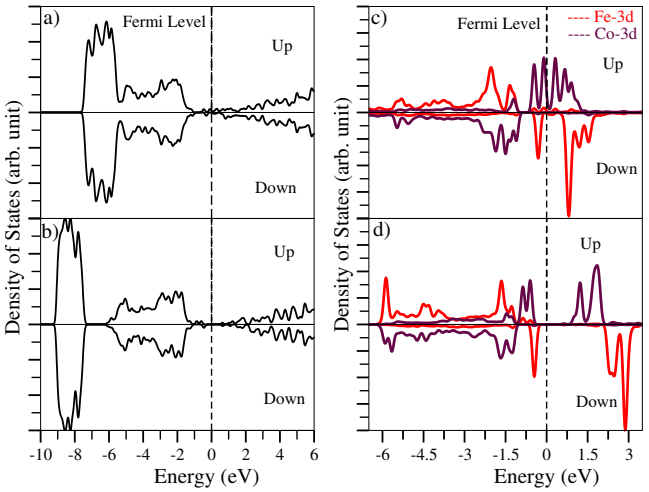

FIG. 5. (Color online) Total and partial density of states for Fe/Co doped in GIIC1 configuration calculated using GGA [(a) and (c)] and GGA+U descriptions [(b) and (d)]. Fe 3d and Co 3d partial density of states are shown by red (gray) and maroon (dark) lines, respectively.

system leads to the incorrect metallic description. However GGA+U method results in a band gap at Fermi level. The total DOS and partial density of states plot for the ground state, i.e., GIIC1 in FiM configuration for Co at $U=2.8$ eV and Fe at $U=3.5$ eV are shown in Figs. 5(b) and 5(d), respectively. Introduction of U separates the partially occupied bands at Fe d and Co d at Fermi level. From DOS [as shown in Fig. 5(d)] for configuration GIIC1 in FiM magnetic state for GGA+U scheme, is clear that Fe is in +2 state at substitutional Zn site and favors high spin ground state with the various level serially filled up as $e\uparrow(2)$, $t_2\uparrow(3)$, $e\downarrow(1)$, and $t_2\downarrow(0)$ (where number in parentheses indicates number of electrons). Also Co is in +2 state when substituted for Zn site and coupled antiparallel to nearest Fe, favors high spin state with the various level serially filled up as $e\downarrow(2)$, $t_2\downarrow(3)$, $e\uparrow(2)$, and $t_2\uparrow(0)$. When Coulomb correlation is included in Fe d orbital half-filled $e\downarrow$ band in minority-spin channel (spin down) splits and occupied part pushed down toward valence band (VB) and unoccupied part pushed up inside the conduction band (CB). In case of Co d orbital occupied and unoccupied Co 3d states in majority-spin channel (spin up), i.e., $e\uparrow(2)$ and $t_2\uparrow(0)$ states are separated by ~ 2.1 eV. Hence at GGA level the electronic structure leads to metallic description while in case of GGA+U level the occupied and unoccupied parts of Fe and Co are separated with proportion of the applied U value. Hence when one Fe and one Co atom are present in the supercell GGA and GGA+U calculation reveals that Fe and Co both preferred to sit on the surface along [0001] direction and coupled antiferromagnetically. While as far as electronic structure is concern GGA+U description is more realistic than GGA description which is consistence with the previous calculation on TM doped ZnO system.[21]

As the ground stat is AFM, the question comes that can we get FM ground state? The possibilities are the following (a) to increase the concentration of Fe and Co and to see which magnetic ground state is preferred, i.e., FM, AFM, or FiM, (b) the role of different charge states, and (c) the role of defects, i.e., Zn vacancy and O vacancy need to be investigated.

Next we have investigated the effect of concentration of Fe and Co impurities in ZnO nanowire. We replaced two pairs of Zn atom with Fe and Co atoms at different sites taking the GIIC1 (where Fe and Co are on cylindrical surface and along [0001] direction) configuration as base and have carried out extensive search for the most favored geometric and magnetic configuration. For this we have considered a longer ZnO naowire generated from $7\times7\times4$ ZnO supercell, containing a total 192 atoms ($Zn_{96}O_{96}$). Next we have constructed different configurations where two Fe and two Co atoms form nearest neighbors these configurations are defined as near tetramer configurations. To obtain the ground-state geometry and favorable spin alignment in near configurations we have taken converged GIIC1 configuration as the initial geometry. First we have replaced one Zn by Fe near to the Fe-Co dimer thus Fe-Co-Fe trimer configurations are generated. We have considered several such possible configurations and calculated the binding energy for each possible configuration. Next separately we have replaced one Zn by Co near to Fe-Co dimer and hence Fe-Co-Co trimer con-

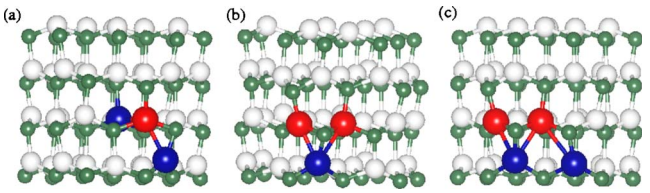

FIG. 6. (Color online) Optimize geometry of (a) FeCoCo, (b) FeCoFe, and (c) FeCoFeCo clusters in ZnO nanowire. The white (lighter) spheres are Zn, dark green (gray) small spheres are O, the red (gray) large spheres are Fe, and the blue (dark gray) large spheres are Co.

figurations are generated (as shown in Fig. 6). The formation energy of the defects was calculated using the following expression.[22–25]

We have calculated the formation energy (E^f) of the different dimer, trimer, and tetramer configurations using the formula,

$$E^f = E[Zn_mO_n(\alpha,q)] - E[Zn_pO_p(\text{pure nanowire})] + \sum n_\alpha \mu_\alpha + q(E_V + \varepsilon_F), \quad (1)$$

where α is the defect atom added or removed from the pure nanowire, n_α is the number of each defect atoms: $n_\alpha = -1(+1)$ for adding (removing) one atom, $E[Zn_mO_n(\alpha,q)]$ is the total energy of the defect in charge state q, $E[Zn_pO_p(\text{pure nanowire})]$ is the total energy of pure ZnO nanowire, μ_α is the chemical potential of the atom α, and ε_F is Fermi level measured with respect to the valence-band maxima (E_V) of pure ZnO nanowire. The chemical potential μ depends on the experimental growth condition. In thermodynamic equilibrium for bulk system, the Zn and O chemical potentials must satisfy the stability condition for ZnO, i.e., $\Delta H\ (ZnO)_{bulk} = \mu_{ZnO} - (\mu^0_{Zn} + \mu^0_O)$, where $\Delta H\ (ZnO)_{bulk}$ is the heat of formation in bulk and determined from the computed total energy of bulk wurtize ZnO, hexagonal closed pack Zn, and molecular O_2. The calculated heat of formation in bulk is −3.44 eV, which is comparable with the experimental value of −3.6 eV.[26] In case of ZnO nanowire chemical potential has been obtained by a condition that $p(\mu^0_{Zn} + \mu^x_{Zn} + \mu^0_O + \mu^x_O) = E[Zn_pO_p(\text{pure nanowire})]$, where μ^x_{Zn} and μ^x_O are defined as excess chemical potential for zinc and oxygen, respectively, and governed by the condition that $\mu^x_{Zn} \leq 0$ and $\mu^x_O \leq 0$ to assure that elementary structure of Zn and O have not formed. The extreme Zn-rich (O-poor) condition is given by $\mu^x_{Zn} = 0$ and extreme O-rich (Zn-poor) condition is given by $\mu^x_O = 0$. For Fe and Co we take both $\mu^x_{Fe} = 0$ and $\mu^x_{Co} = 0$. Chemical potential for Fe is calculated as the energy per Fe atom of cubic crystal structure and chemical potential for Co is calculated as energy per Co of hcp crystal structure. All formation energies are calculated using GGA+U method.

From Fig. 7(a), we find that formation energy of substitutional pair Fe-Co in neutral charge state (GIIC1 configuration in FiM ground state) in Zn-rich condition is 3.57 eV while in O rich the value is −0.98 eV. According to the definition positive value of formation energy means energy is required to incorporate Fe/Co in ZnO nanowire. Thus the formation of Fe-Co defect is more likely to be formed in O-rich condition.

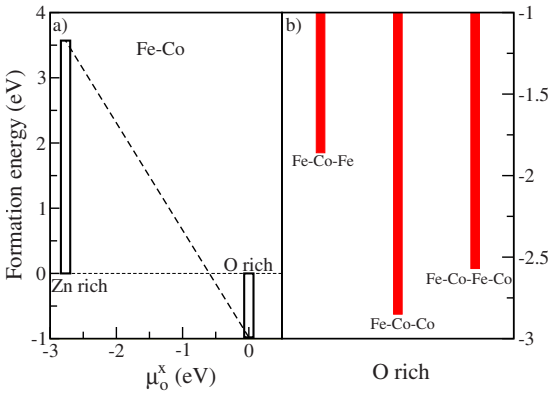

FIG. 7. (Color online) (a) Variation in formation energy of Fe-Co defect in ZnO nanowire with oxygen excess chemical potential at both Zn-rich and O-rich growth conditions, as shown by unfilled bars and (b) comparison of formation energy of Fe-Co, Fe-Co-Co, and Fe-Co-Fe-Co defect configurations at O-rich growth condition, shown as filled red (gray) bar.

In Fig. 7(b), we have shown the formation of all other trimer and tetramer substitutional defects in O-rich condition with respect to Fe-Co formation energy in O-rich condition. The ground-state Fe-Co, Fe-Co-Fe trimer, Fe-Co-Co trimer, and Fe-Co-Fe-Co tetramer configurations are shown Fig. 5. Formation energy Fe-Co-Fe trimer, Fe-Co-Co trimer, and Fe-Co-Fe-Co tetramer (near) configurations are 1.86, 2.85, and 2.57 eV lower in energy that Fe-Co pair formation energy. This shows that the E^f of trimer configurations are less compare with dimer, hence less energy will be required to substitute Fe/Co atoms for Zn close to Fe-Co dimer. Thus third impurity wants to form trimer cluster with the Fe-Co dimer on the cylindrical surface in ZnO nanowire. The ground-state spin configuration for both Fe-Co-Fe and Fe-Co-Co is ferrimagnetic ($\uparrow\downarrow\uparrow$;FiM) with net magnetic moment of 5.0 μ_B and 4.0 μ_B, respectively. This shows that Fe atoms are tend to couple ferromagnetically whereas Co atoms tend to couple antiferromagetically.

To investigate the formation of tetramer cluster keeping Fe and Co concentration same, first we have taken the all Fe-Co-Fe configurations and replace one Zn near to it by Co it this leads to Fe-Co-Fe-Co tetramer configurations. Similarly taking Fe-Co-Co configurations and substituting one Zn near to the defect by Fe leads to Fe-Co-Co-Fe tetramer configurations. It is interesting to note that the ground-state geometry is a Fe-Co-Fe-Co tetramer configuration on the cylindrical surface of ZnO naowire and consists of two Fe-Co dimers and have lowest formation energy when compared with other tetramer cluster configurations. Further we have consider the configuration where two pairs of Fe-Co dimers are on the surface along [0001] direction and are 10.45 Å apart from each other. This configuration is generated by doubling the GIIC1 unit cell and defined as far configuration. This configuration is 0.85 eV higher in energy than near tetramer configuration which implies that Fe-Co has a tendency to form cluster. Also it is interesting to note that the formation energy of Fe-Co-Co trimer configuration is lower in energy when compare to Fe-Co-Fe trimer and Fe-Co-Fe-Co tetramer configurations. This implies that it is difficult

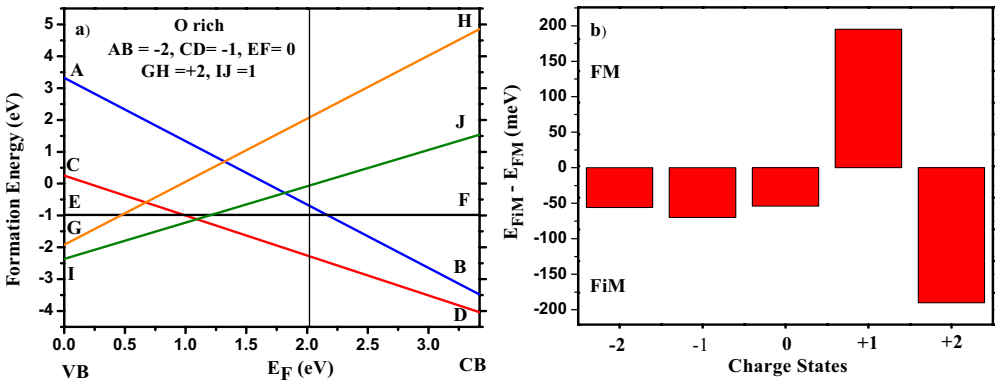

FIG. 8. (Color online) (a) Formation energy of different charge state of Fe-Co defect in ZnO nanowire at O-rich growth condition. Blue (AB), red (CD), black (EF), orange (GH), and green (IJ) line represent variation in formation energy for charge states −2, −1, 0, +2, and +1, respectively, and (b) magnetic exchange interaction energy $[\Delta E = E_{\mathrm{FiM}} - E_{\mathrm{FM}}]$ for different charge state of Fe-Co defect in ZnO nanowire. Shown as red (gray) filled bar.

to keep the same type of atoms away from each other and there is a strong tendency that Co atoms will try to form cluster around a Fe atom which will suppress the ferromagnetic coupling. Previous density functional calculations also shows that Co have a strong clustering tendency when incorporated in ZnO matrix.[27] This tendency will form separate magnetic centers of Fe,Co clusters of different Fe,Co concentration. It will be interesting to investigate how these magnetic centers interact with each other; on the other hand experimentally it is still not clear that how frequent the different transition metals form nearest neighbors sites when compare with the same type in codoped case.

The favorable spin state of Fe-Co-Fe-Co tetramer configuration is ferrimagnetic coupling ($\uparrow\downarrow\uparrow\downarrow$;FiM), which has a total magnetic moment of 2.00 μ_B. The magnetic moment on each atom is 3.556, −2.482, 3.507, and −2.525. The ($\uparrow\downarrow\uparrow\downarrow$;FiM) spin state is 0.096 eV, 0.031 eV, 0.281 eV, 0.358 eV, 0.338 eV, and 0.059 eV lower in energy than ($\uparrow\uparrow\uparrow\uparrow$;FM), ($\uparrow\uparrow\downarrow\downarrow$;AFM), ($\downarrow\uparrow\uparrow\uparrow$;FiM), ($\uparrow\downarrow\uparrow\uparrow$:FiM), ($\uparrow\uparrow\downarrow\uparrow$;FiM), and ($\uparrow\uparrow\uparrow\downarrow$;FiM) states, respectively. From the above discussion we can conclude that FiM is energetically preferred over FM state for Fe/Co clusters for more than two Fe/Co atoms. Hence from the preceding discussion shows that Fe/Co codoped ZnO nanowire is unlike to stabilize in ferromagnetic ground state.

As shift of the Fermi level of Fe-Co doped ZnO nanowire with respect to pure nanowire reveals that impurities lead to an electronic doping effect, hence we have considered different charge state of Fe/Co defect in ZnO nanowire and find out which is the most stable under varying condition. Formation energies of all the charge states of Fe-Co defect at both O-rich growth conditions are shown in Fig. 8(a) and corresponding magnetic exchange energies (i.e., E_{FM} vs E_{FiM}) in Fig. 8(b). We found that +1 charge state of the defect can promote FM.

From the preceding discussion we can conclude that in Fe/Co codoped ZnO nanowire intrinsic FM is unlike and additional carriers are needed to promote FM. In order to understand the observed FM in recent experiment by Liu *et al.*[6] on Fe/Co codoped ZnO nanowires we also explored the possibility of carrier mediated exchange interaction via (a) Zn vacancy or (b) O vacancy. In case of vacancy calculations neutral as well as charge states of the defect complex have been considered in GIICI defect configuration and geometry optimization for both FM and FiM for all the cases have been performed by GGA+U. In case of Zn vacancy, vacancy sites has been considered near to the Fe-Co defect while in case of O vacancy we have considered O vacancy far from the defect and Fe-V_O-Co defect configuration created by removing O atom from Fe-O-Co magnetic path. Here by far, we mean at such distance we can have considerable magnetic coupling, if a defect is created too far from the Fe-Co pair then by using first-principles tools we will not get considerable coupling and ΔE, i.e., $E_{\mathrm{AFM}} - E_{\mathrm{FM}}$ will near equal to zero; also in case of Group-I, i.e., when Fe-Co pair is in the bulk we have considered the V_O vacancy defect in the bulk and for GII, GIII, and GIV configurations, i.e., when Fe-Co pair in on the surface or surface-subsurface interface we have created the defect on the surface. For the defect complexes we have considered all the possible charge state and we have tried to find out which is more favorable under varying condition. In Figs. 9(a) and 9(b) we have shown the formation energies of all the defect complexes in for O-rich growth condition and Zn-rich growth condition, respectively. In Fig. 10, corresponding magnetic exchange energies (i.e., E_{FM} vs E_{FiM}) are shown for the configuration GIICI with Zn vacancy (near), O vacancy (far and on the surface), and Fe-V_O-Co defect complex, respectively.

In case of Zn vacancy we have not found any FM ground state in GIICI configuration. Interestingly O vacancy far from the defect in GIICI configuration is FiM while for Fe-V_O-Co defect complex we have FM coupling for all charge states. However which one of these defect complexes is favorable in terms of formation energy that depends on the growth condition. In O-rich growth condition Zn-vacancy defects are lower in formation energy and in Zn-rich growth condition O vacancy related defects are lower in formation energy. The formation energy of neutral O vacancy at far has lower formation energy compare to Fe-V_O-Co defect complex; however it is interesting to note that for +1 and +2 charge state Fe-V_O-Co defect is lower in formation energy at VB site and −1 and −2 charge state of Fe-V_O-Co is lower in

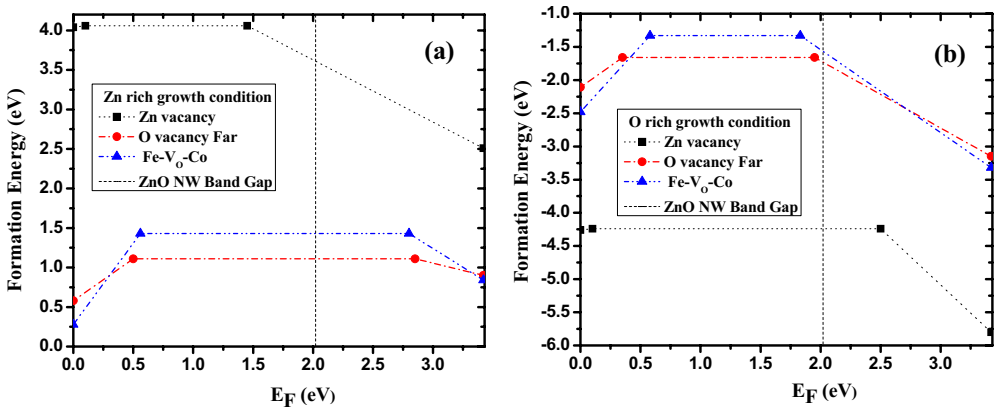

FIG. 9. (Color online) Formation energy of Zn vacancy, O vacancy far, and Fe-V_O-Co defect at both (a) Zn-rich and (b) O-rich growth conditions. Lowest formation energies are only plotted. Zn vacancy, O vacancy far, and Fe-V_O-Co defect complexes are shown by black, red (gray), and blue (dark) lines, respectively.

formation energy at CB site for both Zn-rich and O-rich growth conditions compare with O vacancy far, however in the later case the difference is small. Thus in Zn-rich growth condition at *p*-type (VB side) doping condition the observed FM is due to the direct exchange of holes in Fe-V_O-Co defect complex and in *n*-type (CB side) doping condition the FM state can be stable by direct exchange of electrons. On the other hand at O-rich growth condition Zn vacancy with +1 charge state is the lowest value of formation energy at *p*-type (VB side) doping condition and −1 charge state is the lowest value of formation energy at *n*-type (CB side) doping condition. However we have not found any FM ordering due to Zn-vacancy related defect in GIIC1 configuration.

The formation energies of different defect complex with varying charge state for different growth conditions are expected to vary with different location of Fe-Co pair. Which one of the defect complex is favorable under varying condition will depend on the fact that where Fe-Co pair is formed, i.e., on the surface, surface-subsurface interface, or in bulk environment. In this communication we have considered the formation of vacancy related defects only for the situation where Fe-Co pair is on the surface and concluded that on the surface Fe-V_O-Co charge state defects complexes have lower formation energy compare to O vacancy created at far.

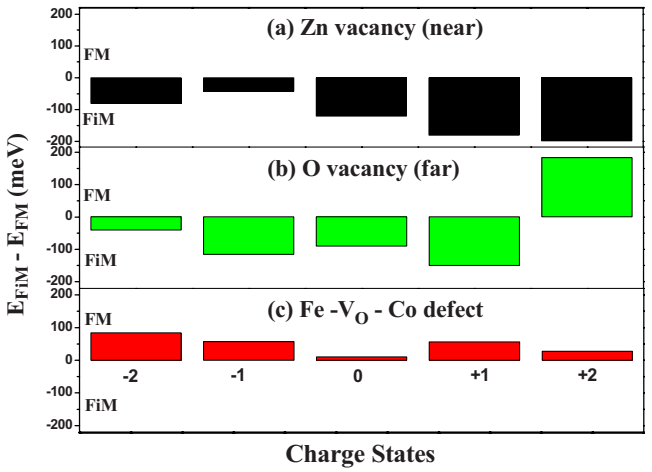

FIG. 10. (Color online) Magnetic exchange interaction energy $[\Delta E = E_{FiM} - E_{FM}]$ of different charge state of Zn vacany, O vacany far, and Fe-V_O-Co defect for GIIC1 configuration. Black (black), green (light gray), and red (dark gray) filled bars represents Zn vacancy, O vacancy far, and Fe-V_O-Co defect complex, respectively.

Next we have extended our study for O vacancy far and Fe-V_O-Co in neutral charge state for all configurations of Fe-Co pair. In Figs. 11(a) and 11(b) variation magnetic exchange energy (ΔE) with Fe-Co all the configurations are shown for both O-vacancies at far and Fe-V_O-Co defect complex at neutral charge state. In case of O vacancy far we have an oscillatory variation, i.e., the sign of the coupling is altered with the Fe-Co separation, i.e., this sign of RKKY type of exchange interaction for the group GI, i.e., when Fe-Co pair is in bulk environment and the O vacancy in created in the bulk. However in case of Fe-Co pair on the surface of the preferred magnetic coupling is always remain FiM when O vacancy is far from the defect and on the surface. We found that Fe-V_O-Co defect configurations (formed by removing the O atom from the Fe-O-Co magnetic path) are ferromagnetic when Co-Fe separation is less than 2.596 Å in GGA scheme and 2.801 Å in GGA+*U* scheme irrespective of the location of transition-metal ions. In case of Fe-V_O-Co defect configurations the Fe-Co bond distances are reduced compared to the Fe-O-Co defect configurations. Previous first-principles calculation reported that Fe-Co pairs are ferromagnetic with a separation of 2.1 Å.[28,29] Hence these results indicate that the competition of RKKY exchange interaction and direct exchange via Fe-V_O-Co is the main competing factor for stabilization of FM in Fe-Co codoped ZnO nanowire.

IV. SUMMARY

In conclusion, we have shown that in Fe/Co codoped ZnO nanowire substitution of Zn by Fe and Co is favorable in O-rich growth condition. The ground-state geometry is found as where Fe and Co are nearest neighbors on the surface along [0001] direction and corresponding magnetic ground state is FiM. Considering all configuration we found that, the

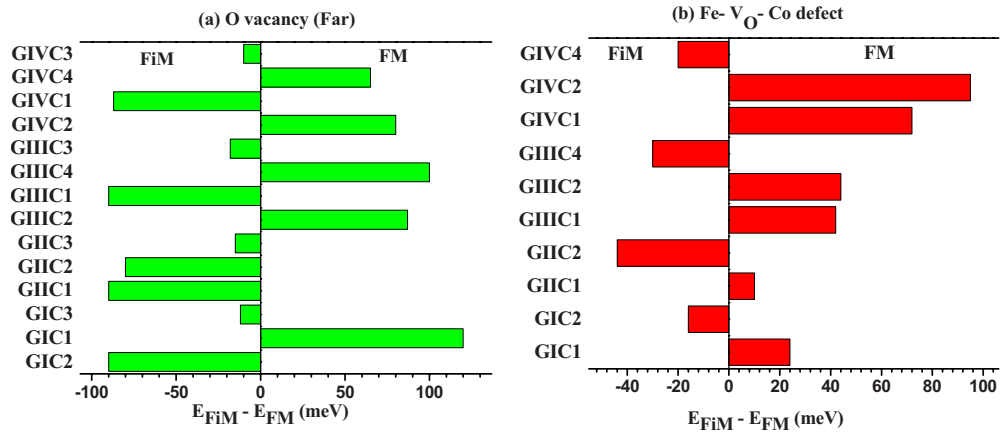

FIG. 11. (Color online) Magnetic exchange interaction energy $[\Delta E = E_{\mathrm{FiM}} - E_{\mathrm{FM}}]$ for (a) O vacancy far, shown as green (light gray) filled bars and (b) Fe-V_O-Co defect, shown as red (dark gray) filled bars for all Fe/Co coped configurations as shown in Fig. 2.

spin alignment between two impurity atoms depends on their location and radial confinement. In GGA description ferromagnetic ordering is observed when impurity atoms sit at surface and subsurface interface forming Fe-O-Co magnetic path. However the magnet ground state altered significantly when GGA+U description is considered. In case of Fe-Co doped ZnO nanowire in neutral charge state the short-range FiM interaction is dominant over double exchange and the magnetic ground state is FiM. Also it is difficult to keep the same type of atoms away from each other and there is a strong tendency that Co atoms will try to from cluster around a Fe atom which will lead to inhomogeneous concentration of Fe and Co and FiM coupling will be the preferred magnetic aliment. When two Fe and Co atoms are considered in the supercell keeping Fe,Co concentration same, the Fe-Co dimer forms cluster on the surface of the nanowire with FiM as magnetic ground state. Intrinsically the system in ferrimagnetic can be altered to fermomagnetic by addition of one hole per Fe-Co pair. In case vacancy related defect when considered ground-state Fe-Co pair configuration where Fe-Co is on the surface, we found only particular defect complex, i.e., Fe-V_O-Co is FM. The formation of defect is depends on the growth condition and expected to depend on the location of Fe-Co pair as well. In case of O vacancy related defect we have two distinct mechanisms which can lead to FM (the two competing mechanism), the RKKY type of exchange interaction in bulk environment and direct exchange interaction of carriers due to Fe-V_O-Co defect configuration on the surface.

ACKNOWLEDGMENTS

We thank the staff of the Center of Computational Materials Science at IMR for the use of Hitachi SR11000-K2 Supercomputing facilities. G.P.D. acknowledges the support from the BRNS (India) under the Spintronics CRP.

*Corresponding author; saurabhghosh2802@gmail.com

[1] S. A. Wolf, D. D. Awschalom, R. A. Buhrman, J. M. Daughton, S. Von Molnar, M. L. Roukes, A. Y. Chtchelkanova, and D. M. Treger, Science **294**, 1488 (2001).
[2] D. M. Bagnall, Y. F. Chen, Z. Zhu, T. Yao, S. Koyama, M. Y. Shen, and T. Goto, Appl. Phys. Lett. **70**, 2230 (1997).
[3] Z. K. Tang, G. K. L. Wong, P. Yu, M. Kawasaki, A. Ohtomo, H. Koinuma, and Y. Segawa, Appl. Phys. Lett. **72**, 3270 (1998).
[4] W. B. Jian, Z. Y. Wu, R. T. Huang, F. R. Chen, J. J. Kai, C. Y. Wu, S. J. Chiang, M. D. Lan, and J. J. Lin, Phys. Rev. B **73**, 233308 (2006).
[5] J. J. Wu, S. C. Liu, and M. H. Yang, Appl. Phys. Lett. **85**, 1027 (2004).
[6] L. Q. Liu, B. Xiang, X. Z. Zhang, Y. Zhang, and D. P. Yu, Appl. Phys. Lett. **88**, 063104 (2006).
[7] J. J. Chen, M. H. Yu, W. L. Zhou, K. Sun, and L. M. Wang, Appl. Phys. Lett. **87**, 173119 (2005).
[8] J. J. Liu, K. Wang, M. H. Yu, and W. L. Zhou, J. Appl. Phys. **102**, 024301 (2007).
[9] X. L. Zhang, R. Qiao, R. Qiu, Y. Li, and Y. S. Kang, J. Phys. Chem. A **111**, 4195 (2007).
[10] Y. M. Cho, W. K. Choo, H. Kim, D. Kim, and Y. E. Ihm, Appl. Phys. Lett. **80**, 3358 (2002).
[11] M. S. Park and B. I. Min, Phys. Rev. B **68**, 224436 (2003).
[12] Q. Wang, Q. Sun, G. Chen, Y. Kawazoe, and P. Jena, Phys. Rev. B **77**, 205411 (2008).
[13] W. Kohn and L. J. Sham, Phys. Rev. **140**, A1133 (1965).
[14] Y. Wang and J. P. Perdew, Phys. Rev. B **44**, 13298 (1991).
[15] G. Kresse and J. Furthmuller, Phys. Rev. B **54**, 11169 (1996).
[16] G. Kresse and D. Joubert, Phys. Rev. B **59**, 1758 (1999).
[17] Q. Wang and P. Jena, Appl. Phys. Lett. **84**, 4170 (2004).
[18] Q. Wang, Q. Sun, Y. Kawazoe, and P. Jena, Appl. Phys. Lett. **87**, 162509 (2005).
[19] S. Lany, H. Raebiger, and A. Zunger, Phys. Rev. B **77**, 241201(R) (2008).
[20] A. Walsh, J. L. F. Da Silva, and S.-H. Wei, Phys. Rev. Lett. **100**, 256401 (2008).
[21] P. Gopal and N. A. Spaldin, Phys. Rev. B **74**, 094418 (2006).

[22] S. Ossicini, E. Degoli, F. Iori, E. Luppi, R. Magri, G. Cantele, F. Trani, and D. Ninno, Appl. Phys. Lett. **87**, 173120 (2005).
[23] P. Mahadevan and A. Zunger, Phys. Rev. Lett. **88**, 047205 (2002).
[24] C. G. Van de Walle and J. Neugebauer, J. Appl. Phys. **95**, 3851 (2004).
[25] N. Ganguli, I. Dasgupta, and B. Sanyal, Appl. Phys. Lett. **94**, 192503 (2009).
[26] F. Tuomisto, K. Saarinen, D. C. Look, and G. C. Farlow, Phys. Rev. B **72**, 085206 (2005).
[27] D. Iuşan, M. Kabir, O. Grånäs, O. Eriksson, and B. Sanyal, Phys. Rev. B **79**, 125202 (2009).
[28] A. N. Andriotis, G. Mpourmpakis, G. E. Froudakis, and M. Menon, J. Chem. Phys. **120**, 11901 (2004).
[29] G. Mpourmpakis, G. E. Froudakis, A. N. Andriotis, and M. Menon, Phys. Rev. B **72**, 104417 (2005).